Effect of cross-linker geometry on equilibrium thermal and mechanical properties of nematic elastomers

S. M. Clarke,* A. Hotta, A. R. Tajbakhsh, and E. M. Terentjev†

Cavendish Laboratory, University of Cambridge, Madingley Road, Cambridge, CB3 0HE, United Kingdom

We study three monodomain (single-crystal) nematic elastomer materials, all side-chain siloxane polymers with the same mesogenic groups but with different types of cross linking: (i) short flexible siloxane linkage affine to the network backbone, (ii) short flexible aliphatic cross links miscible with mesogenic side chain groups, and (iii) long segments of main-chain nematic polymer. Equilibrium physical properties of these three systems are very different, especially the spontaneous thermal expansion and anisotropic stress-strain response along and perpendicular to the uniform nematic director. In the latter case, we examine the soft elastic plateau during the director reorientation. We compare the nematic order-parameter $Q(T)$, provided primarily by the side mesogenic groups and relatively constant between the samples, and the average backbone chain anisotropy $r(T) = \ell_\parallel / \ell_\perp$, which is strongly affected by the cross-linking geometry. The experimental data are compared quantitatively with theoretical models of nematic elastomers.

PACS number(s): 61.30.−v, 61.41.+e, 83.60.Bc

I. INTRODUCTION

In recent years, the behavior of liquid crystalline elastomers has been the subject of significant experimental and theoretical interest. The behavior of these materials arises from a coupling between the liquid-crystalline ordering of mesogenic moieties and the elastic properties of the polymer network. Many unusual physical effects have been identified and reported in review articles [1–4]. The origin of this equilibrium behavior has been extensively studied theoretically, within a molecular model of ideal and nonideal nematic network [5]. A more recent development allowed us to combine the concepts of reptation theory of entangled networks with the anisotropic nature of nematic polymer strands [6], obtaining the "tube model" corrections to the ideal nematic rubber elastic free energy.

Two key equilibrium effects stand out in the properties of liquid-crystalline elastomers, being especially pronounced when a monodomain (single crystal, permanently aligned [7]) nematic network is prepared. The first effect is the anomalous thermal expansion—the spontaneous elongation of the material along the director axis on cooling from the isotropic phase [8,9]. The reason for this phenomenon is in the direct coupling between the average polymer chain anisotropy and the nematic order parameter (see, e.g., [5] for detail). Depending on this coupling, the magnitude of thermal expansion may differ greatly (and even change sign in a polymer with oblate backbone conformation), reaching a maximum in a main-chain nematic polymer systems that could expand, spontaneously and reversibly, by a factor of three or more [10]. The other effect, a macroscopic phenomenon termed the "soft elasticity" [11], determines the equilibrium mechanical and optical responses of monodomain

nematic elastomers, as well as the properties of polydomain-monodomain transition [12]. The physical idea behind soft elasticity is again in the spontaneous anisotropy of polymer backbones of rubbery network, coupled to mesogenic moieties that align and form the nematic order. In conventional elastomers and gels it is the entropic cost of deforming the average (spherical) backbone polymer coil that provides the restoring force and elasticity. When the network strand is anisotropic (ellipsoidal), then instead of deforming the average polymer conformation, some deformations could be completely accommodated by simply rotating the average chain distribution without changing its shape. Accordingly, no elastic energy cost would be paid for such deformations. In many cases, the ideal soft response cannot be achieved, but one still finds a signature of soft elasticity in the decrease of one of the shear moduli for the same deformation modes that would lead to a complete softness in an ideal nematic network.

Here, we examine these two physical effects in some detail. We study three types of nematic elastomer materials, having essentially the same chemical structure and composition of side-chain polysiloxane nematic polymer strands but different in the type of cross linking. We establish the network using exactly the same concentration (by reacting bonds) of difunctional cross-linking groups that are (i) short flexible dimethylsiloxane chains, (ii) hydrocarbon divinyl alkenebenzene units, and (iii) long chains of main-chain nematic polymer that create an additional (and very high) anisotropy in the composite material. In all cases, we prepare uniformly aligned monodomain nematic networks—single-crystal liquid-crystal elastomers in the terminology of Küpfer and Finkelmann [7].

There are several questions to answer from comparing these three systems. First, in Sec. III, we establish a relation between the nematic order-parameter $Q(T)$ and the effective backbone anisotropy of chains making the rubbery network, expressed by a dimensionless ratio of principal step lengths along and perpendicular to the nematic director, $r = \ell_\parallel / \ell_\perp$. It is obvious that there has to be a direct relation-

---

ship, with the limit $r \rightarrow 1$ at $Q \rightarrow 0$. However, the theoretical derivation of such a correspondence is strongly model dependent, varying from a trivial $r = (1+2Q)/(1-Q)$ for a freely jointed chain of rods to a highly nonlinear $r \propto \exp[3/(1-Q)]$ in the hairpin regime of main-chain homopolymers [13]. The results for the correlation between $r(T)$ and $Q(T)$ variations across the nematic clearing point in the three materials demonstrate that, although the principal nematic order is essentially the same (which would be expected, as it is formed by mesogenic groups identical in structure and concentration), the effective mechanical anisotropy $r(T)$ of network strands is vastly different. To understand this, one needs to revise the concept of the backbone anisotropy and introduce a separate order parameter—the nematic order of the polymer backbone, Q_b. For a freely jointed chain of rods, $Q \equiv Q_b$, but in a real material, the difference in magnitude (and even the sign) could be great. Nevertheless, a good linear relationship between their optical and mechanical anisotropies is found, which we further discuss at the end of this paper.

In Sec. IV, we present results of quasiequilibrium stress-strain measurements for the three materials. When stretched along the uniform nematic director, the nematic elastomer responds to deformation linearly, with a characteristic extension (Young) modulus $E_{\parallel}$ of an incompressible polymer system. Stretching perpendicular to the director induces the director reorientation, via the stripe domain regime [5,14] with a characteristic stress plateau indicating that all our materials have rather low degrees of semisoftness. We used the term "quasiequilibrium" in this context, because the results significantly depend on the rate of imposed deformation. The slow relaxation of stress in nematic elastomers [15] is most pronounced when structural changes occur in the director texture. Our measurements clearly indicate the role of slow relaxation when internal changes occur in the director field; both the range of stress plateau and the relaxation time increase dramatically with increasing backbone anisotropy in the main-chain containing elastomers.

Finally, in Sec. V, we conclude with a discussion of theoretical concepts that could be applied to describe experimental results. We also speculate about the possible applications, in particular, in thermomechanical actuators. There are competing factors, for instance, the amplitude and the steepness of the response are in the opposite relation to the response rate. Comparing the three materials that span the whole range of possibilities, we propose that highly anisotropic main-chain containing nematic elastomers are most suitable for large-amplitude (or large force) actuation when the time is a less relevant factor, while the low-anisotropy nematic materials provide the low-amplitude but high-frequency response suitable, for instance, for acoustic applications.

II. EXPERIMENT

Samples of side-chain siloxane liquid crystalline elastomers were prepared in the Cavendish Laboratory following the procedure of Küpfer and Finkelmann, and Finkelmann *et al.* [7,16], with three different cross linkers. The polymer
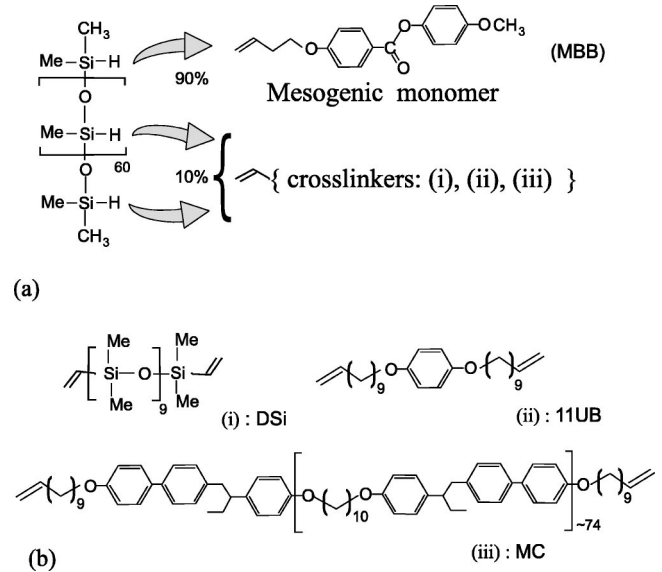

FIG. 1. Schematic illustration of the materials used in this paper. (a) Siloxane backbone chain with Si-H groups reacting with 90 mol % mesogenic phenyl-benzoate side groups, MBB, and 10 mol % of divinyl cross-linking groups: (b) flexible siloxane chain, DSi (giving the SiF sample), flexible small-molecule 1,4 alkeneoxy-benzene, 11UB (resulting in the SiH material), and the main-chain nematic polymer of 1-biphenyl-2-phenyl butane, MC (giving the two SiMC materials).

backbone was a poly-methylhydrosiloxane with approximately 60 Si-H units per chain, obtained from AGROS Chemicals. The pendant mesogenic groups were $4'$-methoxyphenyl-4-(1-buteneoxy) benzoate (MBB), as illustrated in Fig. 1, attached to the backbone via the hydrosilation reaction.

All networks were chemically cross linked via the same reaction, in the presence of a commercial platinum catalyst COD, obtained from Wacker Chemie, with difunctional cross-linking groups also shown in Fig. 1. In all cases, the cross-linking density was calculated to be 10 mol % of the reacting bonds in the siloxane backbone, so that on average, each siloxane chain has nine pendant mesogenic groups between cross-linking sites. Three cross-linking agents were the following: (i) A short (nine-unit) flexible chain of divinyl terminated polydimethylsiloxane, an extension of the siloxane backbone (DSi, from AGROS Chemicals). (ii) A carbohydrate 1,4 di(11-undecene) benzene (11UB), a small flexible molecule deemed to have a relatively minor effect on the overall mesogenic properties of the liquid-crystalline polymer (synthesized in the house). The third cross-linking agent was very different: (iii) di-vinyl terminated chains α-{4-[1-(4'-{11-undecenyloxy} biphenyl)-2-phenyl] butyl}-ω-(11-undecenyloxy) poly-[1-(4-oxydeca methyleneoxy)-biphenyl-2-phenyl] butyl polymers (MC) that themselves make a main-chain liquid crystal [17]. In our case the cross-linking chains were with ~ 74 rodlike monomers between the terminal vinyl groups (determined by GPC, polydispersity ~ 2). Each such long-chain cross linker connects two siloxane polymer chains. These three elastomers were prepared from the same batch of backbone and side-group

TABLE I. Proportions (in mol %) of cross-linkers DSi, 11UB, and MC in the overall cross-linking composition (of the fixed total of 10%), the corresponding volume fraction of the side-chain mesogenic polymer (in wt %), and temperatures of glass and nematic-isotropic transitions. The glass transition temperatures are approximate, with an error of at least $\pm 5°$.

Samples	%(DSi)	%(11UB)	%(MC)	SC weight	T_g (C)	T_{ni} (C)
SiF	10	0	0	78%	-3	68
SiH	0	10	0	87%	3	86
SiMC	0	9	1	42%	2	107
SiMC10	0	0	10	7%	17	108

mesogenic materials, with the same relative concentration of cross-linking groups.

Calculating the cross-linking density by reacting bonds, as described above, can be quite different from the actual concentration of the species in resulting material. In particular, in the case of MC polymer cross linker, the relative gram weight of it in the otherwise side-chain polymer matrix is very high: the molecular weight of an average MC cross-linking chain, cf. Fig. 1, is $34\,530 = 75 \times 456$—which is much greater than the molecular weight of the corresponding nine-unit side-chain polymer strand between cross-linking points ($2691 = 9 \times 299$). One may equally regard such a system as a *main-chain nematic rubber network*, end linked with relatively small cross-linking groups made of side-chain nematic polysiloxane. In a different study [10], we have found an optimal proportion of MC cross linker that has the characteristic high anisotropy of main-chain nematic polymer, but has a response time sufficiently fast for meaningful experiments. This composition is close to the borderline when the overall mass of MC material in the network is approximately equal to that of side-chain polysiloxane, that is a cross linking by a combination of approximately 1 mol % of MC and 9 mol % of 11UB. The materials, synthesized in this way, are referred to as SiF, for the flexible siloxane cross linking, SiH for hydrocarbon rodlike cross-linking groups, and SiMC for cross linking via the main-chain nematic polymer; there are two MC-containing materials—the ''optimal'' composition of {one part MC and nine parts 11UB}, and the fully MC-cross-linked network, named SiMC10. The cross-linking composition of these materials is listed in the Table I, together with the actual concentration of side-chain mesogenic material in the overall network. Characteristic transition temperatures are also given in this table. One can clearly see an effect of composition on the N-I transition temperature, which is to be expected for such chemically different cross links acting as effective impurities.

Monodomain, aligned samples were made by preparing partially cross-linked films in a centrifuge, highly swollen in toluene (2–3 ml per 1 g of material), reacting for 25–35 min before evaporating the solvent and suspending the samples under load in an oven to complete the reaction for more than five hours at 120 °C. A careful study of reaction kinetics ensured that approximately 50% of cross links were established in the first stage of this preparation. When a uniaxial stress is applied to such a partially cross-linked network, the aligned monodomain state in the resulting nematic elastomer is established with the director along the stress axis. This orientation is then fixed by the subsequent second-stage reaction, when the remaining cross links are fully established. Note that the final cross-linking temperature is in the isotropic phase of all materials. Following the ideas and results of [7], in all cases we performed the second-stage cross linking in this high-temperature phase: in this way, a better alignment and mechanical softness are achieved (in contrast to the cross linking in a stretched polydomain nematic phase [7,12], which results in a number of defects and domain walls frozen in the material).

Equilibrium transition temperatures given in Table I were determined on a Perkin Elmer, Pyris 1 differential scanning calorimeter, extrapolating to low cooling rates, and the nematic phase identified by polarizing optical microscopy and x-ray scattering. Thermal expansion measurements were made by suspending the samples, without load, in a glass-fronted oven and measuring the variation in natural length of the samples with temperature, $L(T)$. Precise length measurements were made using a traveling microscope, as the samples were slowly cooled (at a rate 0.5°/min) after complete annealing in the isotropic state.

The force measurements were performed on a custom-built device consisting of a temperature-compensated stress gauge and controller (UF1 and AD20 from Pioden Controls Ltd) in a thermostatically controlled chamber (Cal 3200 from Cal Controls Ltd). The long strips of rectangular-shaped samples were mounted with clamps, at room temperature, in such a way that the sample length L remains fixed throughout the experiment. The samples were then heated (at a rate $\sim 0.5°$/min) to the isotropic phase. The stress and temperature values were acquired by connection to a Keithley multimeter (2000 series) and stored on a PC over an IEEE interface. Data obtained in arbitrary units were converted to nominal stress in units of N/mm$^2 = 10^6$ Pa by calibration with weights. The issues of long-stress relaxation and thermal stability are always important in liquid-crystalline elastomers. All mechanical experiments were performed at two slow strain rates of ~ 0.004 s^{-1} and $\sim 10^{-5}$ s^{-1}, verifying that there has not been any noticeable variation in the (assumed equilibrium) stress readings. This requirement has not been satisfied for the SiMC10 material, whose relaxation rates are very slow—hence, we did not include its nonequilibrium stress-strain data in this paper. Since the natural length L_0 of monodomain nematic elastomer is a very sensitive function of temperature, any meaningful measurement of equilibrium stress response must be performed at a fixed and carefully maintained temperature.
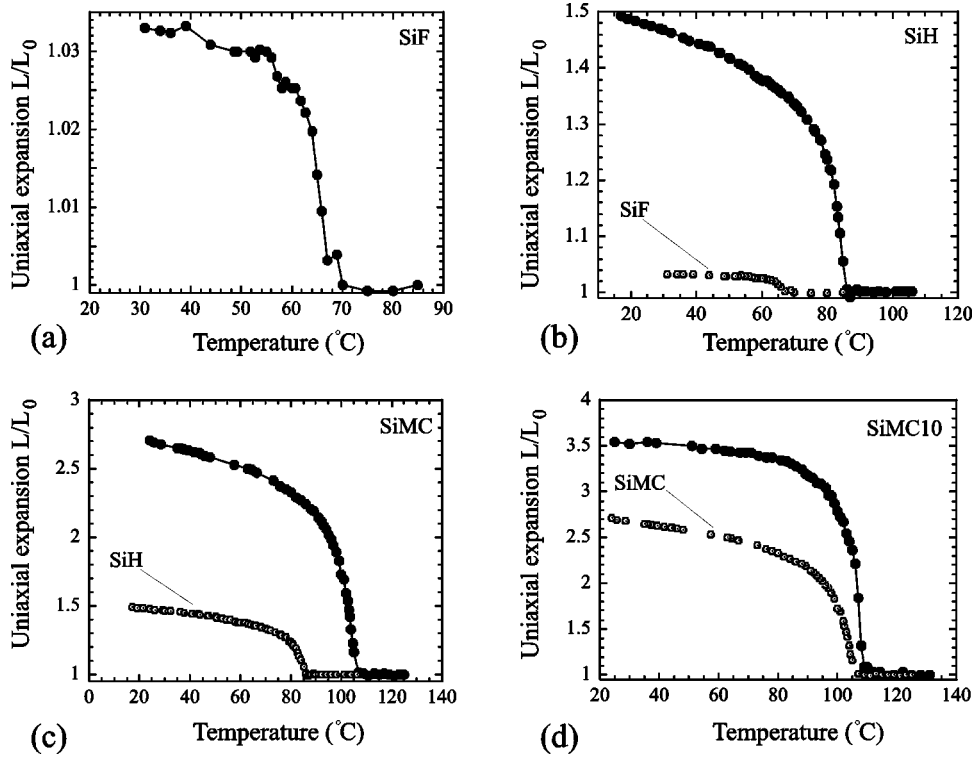
FIG. 2. Thermal expansion data for three polysiloxane monodomain nematic elastomers: SiF, SiH, SiMC, and SiMC10 (labeled on the plots). The data present the spontaneous uniaxial strain $\lambda_{th} = L/L_0$ on cooling of freely suspended rubber strips. All samples, except SiMC10, were cooled at a rate $\sim 0.5°/\text{min}$; the fully MC material is proven very slow to respond and required a much lower rate (below $0.2°/\text{min}$ in the region of the transition)—even then we were not confident in that the sample has equilibrated at each temperature value.

III. THERMAL PROPERTIES

Figure 2 presents the thermal expansion data for the samples SiF, SiH, SiMC, and SiMC10. The data represent the spontaneous change in length of the sample along the uniform nematic director, which occurs on changing the temperature and, accordingly, the underlying nematic order. The measured length $L(T)$ is normalized with respect to the sample length L_0 obtained in the isotropic state above the nematic transition temperature T_{ni}. The theory of equilibrium ideal nematic elastomers [5] identifies this spontaneous deformation $\lambda_{th} = L/L_0$ with the effective mechanical anisotropy of polymer backbones of the network. This anisotropy is directly experimentally measured as, for instance, the ratio of principal radii of gyration $R_\parallel / R_\perp$ (see, e.g., [18]). The theory uses the parameter $r = \ell_\parallel / \ell_\perp$, the ratio of principal step lengths of the ideal nematic network strand (equally, $r = (R_\parallel / R_\perp)^2$ for the principal gyration radii) and obtains the spontaneous deformation $\lambda_{th} = r^{1/3}$. In this context, the term "ideal" refers to the simplest case of Gaussian polymer network with uniaxial average backbone anisotropy. In more complex, nonideal elastomers, the relation between the parameter r, calculated from the uniaxial thermal expansion $[L(T)/L_0]^3$, and the principal chain step lengths may be less clearly defined. Nevertheless, the single parameter of theory, $r(T)$ has to be a function of nematic order; in the isotropic phase; above T_{ni} one has $r = 1$.

Figure 2 presents the plots of L/L_0 in a sequence, because the magnitude of spontaneous strain $\lambda_{th}(T)$ is very different. For comparison, the plot in Fig. 2(b) for SiH has the SiF data as well, similarly the plot in Fig. 2(c) for SiMC has the SiH data and the plot in Fig. 2(d) for SiMC10 has the SiMC data from the previous corresponding graph.

The effective mechanical anisotropy r of each network

should be calculated as the cubic power of $\lambda_{th}(T)$. One is impressed by the great variation of this measure between our materials. In SiF (an ordinary polysiloxane nematic elastomer, cross linked by short flexible segments of polysiloxane chains) the value of r reaches only ~ 1.1 deep in the nematic phase. This would correspond to the ratio of radii of gyration $R_\parallel / R_\perp \sim 1.05$, if we assume that r directly reflects the chain step length anisotropy. In a very similar material SiH, with the only difference that it is cross linked by short flexible carbon chains, the value of r reaches ~ 3.3 (the same as reported earlier by Kundler and Finkelmann and Finkelmann *et al.* [14,16]), corresponding to $R_\parallel / R_\perp \sim 1.8$. When the network also contains a main-chain nematic polymer, the effective anisotropy is much greater: $r \sim 20$ for SiMC and $r \sim 43$ for SiMC10. The latter would correspond to $R_\parallel / R_\perp \sim 6.5$, favorably comparing with the neutron-scattering data on main-chain polymer melts [19].

The sharp break in each curve $\lambda_{th}(T)$ clearly indicates the clearing transition temperature T_{ni}, which is in a good agreement with DSC measurements given in Table I. For all samples, the increase in length along the nematic director, as the samples are cooled below the clearing transition temperature, indicates the average prolate anisotropy of polymer backbones induced by the increasing nematic order (that is, $R_\parallel > R_\perp$). In a monodomain nematic rubber, all these chains are oriented on average with the long axis of their ellipsoidal shape of gyration aligned with the nematic director, uniformly along the sample. On heating through the clearing transition, where the mesogenic influence is lost, the backbone polymer coils return to the isotropic spherical average shape. It is this change in polymer backbone conformation that gives rise to the dramatic thermomechanical behavior of nematic rubber illustrated in Fig. 2.
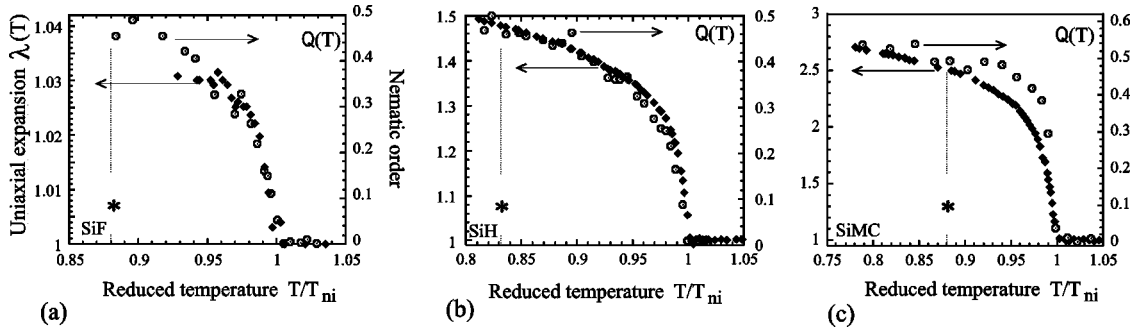
FIG. 3. The spontaneous uniaxial strain $\lambda_{th} = L/L_0$, increasing on cooling, is plotted together with the nematic order-parameter, $Q(T)$. Three samples, SiF, SiH, and SiMC, show a direct relationship, expressed by the linear function $\lambda_{th} = 1 + \alpha Q$, but with a very different slope: the fitting gives $\alpha = 0.08, 1.02, 2.8$ for the three samples, respectively. On each plot, the star labels the point at which the mechanical experiments of the next section were performed.

The variation in nematic order-parameter $Q(T)$ with temperature for the three samples SiF, SiH, and SiMC, has been obtained from the analysis of azimuthal variation of wide-angle x-ray scattering intensity. The nematic order is formed by side-chain mesogenic groups aligning on average, below T_{ni}, along the unique direction provided by the stress during second-stage cross linking. This order is established on the characteristic nematic coherence length scale $\xi_N \sim 10$ nm. In all materials, the order-parameter $Q(T)$ varied from 0 to ~ 0.6 at low temperature. Figure 3 brings together plots of temperature variation $Q(T)$ and that of spontaneous uniaxial thermal expansion $\lambda = L/L_0$, for SiF, SiH, and SiMC. The correspondence between these two parameters, obtained from very different measurements, is quite spectacular. There is a direct linear relationship, $\lambda_{th} \approx 1 + \alpha Q$, with a strongly varying slope: for weakly anisotropic elastomer SiF is $\alpha \approx 0.08$, for SiH we find an almost exact equality $\alpha \approx 1.02$ and the highly anisotropic SiMC has the slope $\alpha \approx 2.8$.

There are deviations from the perfect linearity in the region of the most steep $\lambda(T)$ variation, for the MC-containing material SiMC. One likely reason for such a deviation is the response time: the long MC chains have a recorded tendency to slow down their dynamics (and even completely freeze [20]) when in the hairpin regime of their nematic conformation. Accordingly, it is plausible that the thermal expansion curve, Figs. 2(c) and 3(c), is not fully equilibrated and lags behind the equilibrium order-parameter increase $Q(T)$. Another possible reason for the discrepancy in the MC-containing material is that the dependence of chain step lengths on Q is highly nonlinear, in contrast to "classical" side-chain liquid-crystalline polymers used in SiF and SiH. We shall return to this issue in the Conclusions section and discuss the implications of a relationship between the main nematic order $Q(T)$ and the induced order of polymer backbones Q_b, which determines $r(T)$ and $\lambda_{th}(T)$.

All subsequent mechanical experiments were performed deep in the nematic phase, between 40 and 50 degrees below T_{ni}, when the order parameter took the value $Q \approx 0.5$.

IV. ELASTIC ANISOTROPY

Equilibrium elastic response of aligned monodomain nematic rubber has been a subject of a number of theoretical and experimental studies over the last years. One finds a crucial difference in applying a uniaxial extension along and perpendicular to the uniform director **n**. When stretched along the axis of anisotropy, the material responds as a classical rubber, showing a linear stress-strain relation over a wide interval of deformations. Recent research [16] addressed an interesting question of linear elastic anisotropy, comparing the rubber modulus at small deformations, for extension in the two perpendicular directions. Obtaining the engineering strain from the imposed extension $\varepsilon = (L - L_0)/L_0$, one identifies the linear Young modulus as a coefficient between nominal stress and small strain $\sigma = E\varepsilon$. The rubber modulus μ is the linear shear modulus, so that $E = 3\mu$ in an incompressible rubber (see Fig. 4). A nontrivial variation of the extension moduli ratio $E_\parallel/E_\perp$ with temperature (and thus nematic order parameter) has been predicted theoretically and observed experimentally by Finkelmann *et al.* [16].

When a uniaxial extension is applied perpendicular to the initial nematic orientation $\mathbf{n}_0$, it induces the director rotation, eventually aligning **n** along the stress axis. Different mechanisms of such director rotation have been reported: a discontinuous 90° jump [21] and a continuous rotation via stripe domains [14]. In all cases, the internal structural relaxation causes a stress plateau, a significant depression in the effective modulus in the region of strains where the director rotation takes place. Only for strains below the semi-soft threshold ε_1 (cf., e.g., [5]), before the rotation starts, can one obtain a proper linear modulus $E_\perp$.

Figure 5 shows the stress-strain plots for uniaxial extension perpendicular to the director of our three materials. In SiF and SiH, the semisoft threshold was rather low and we could not reliably identify this initial linear stress-strain regime. Accordingly, the value of stress on the soft plateau was low as well. For low-anisotropy SiF, we suspect that the director has rotated at very low strain and the data points in Fig. 5(a) correspond to the past-transition region, essentially stretching along the new orientation of **n** (not surprisingly, the slope of this plot $\tilde{E} \approx 11$ kPa is very close to the value of $E_\parallel$ for this material). The initial value $E_\perp \approx 12$ kPa for SiH, determined from the first few data points in Fig. 5(b), is quite unreliable. On the other hand, the highly anisotropic SiMC
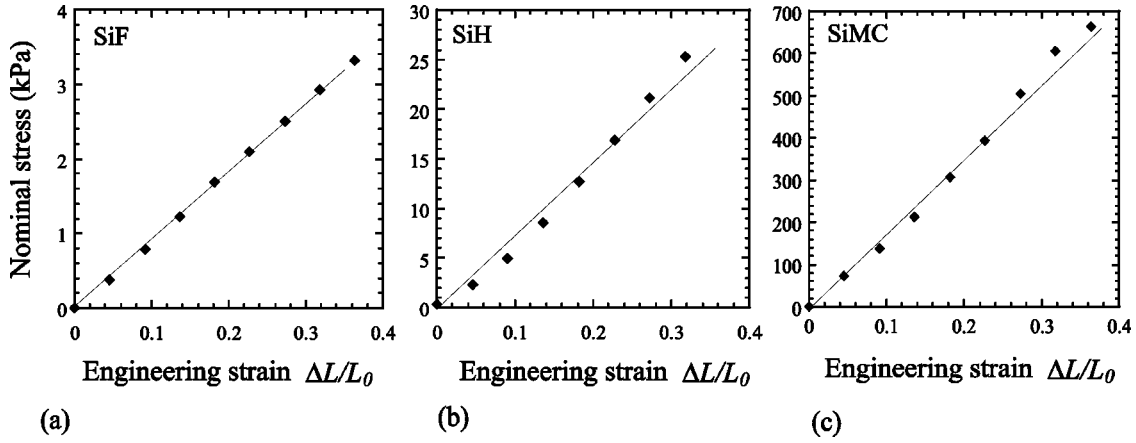
FIG. 4. Stress-strain curves obtained by stretching monodomain nematic elastomers along the nematic director, for each of the three samples: SiF (at 24C, $T/T_{ni} = 0.88$), SiH (at 30C, $T/T_{ni} = 0.83$), and SiMC (at 60.9C, $T/T_{ni} = 0.88$). No director rotation is induced in this geometry. The slopes of each linear plot give the Young modulus $E_{\parallel}$ for SiF: 9 kPa, SiH: 75 kPa and a much higher value for SiMC: 1.8 MPa.

shows an unambiguous linear regime before the threshold, giving $E_{\perp} \approx 0.86$ MPa and the threshold strain $\varepsilon_1 \approx 0.45$. This is the only case where we can reliably report the elastic anisotropy value $E_{\parallel}/E_{\perp} \approx 2.1$ at $Q \approx 0.5$.

The theory [5] also predicts the value of strain at which the rotation is complete and the director is aligned along the axis of applied stress. In present notation, when the engineering strain is defined as $\varepsilon = \Delta L/L_0$, the soft plateau ends at $\varepsilon_2 \approx (1 + \varepsilon_1)\sqrt{r} - 1$. For SiF, with $r \equiv \lambda_{th}^3 \approx 1.1$, the end of director rotation regime should be around $\varepsilon_2 \approx 0.05$, below the resolution of our device. For SiH, with $r \approx 3.2$ and estimated threshold $\varepsilon_1 \approx 0.05$, the predicted end of the soft plateau would be at $\varepsilon_2 \approx 0.88$—not dissimilar to the actual measured data in Fig. 5(b). For SiMC, the effective anisotropy is very high, $r \approx 30$, resulting in the estimated end of the soft plateau at $\varepsilon_2 \approx 4.73$. Such an incredibly long interval of estimated strains for the soft plateau is consistent with the data of Fig. 5(c).

V. CONCLUSIONS

In this short paper, we demonstrate the anisotropic mechanical behavior of three liquid-crystalline elastomers with different type of cross linking. Composite materials SiF, SiH, and SiMC combined main-chain and side-chain nematic polymers and different linking mechanisms in their networks. The results are sensitive functions of the way networks are cross linked. Increasing the proportion of MC in the otherwise side-chain nematic network has a great effect on the average effective anisotropy of polymer chains and, as a result, on the magnitude of spontaneous strain λ_{th}. On the other hand, networks cross linked by siloxane linkers have very low-mechanical anisotropy and practically no soft stress regime on stretching perpendicular to **n**.

We also note the correlation between the effective network anisotropy $r(T)$ and the rate of mechanical relaxation. SiF has very short relaxation time, and SiH is responding reasonably fast too: we see no hysteretic effects at our cooling or strain rates. There is a pronounced slowing down of all response processes with the addition of highly anisotropic MC. In the material SiMC10, with nearly half of the mass taken by the MC polymer, we were unable to reach the mechanical equilibrium at our laboratory time scales. The compromise has been found in the SiMC composition (with only 1 mol % of MC in the overall 10% cross linking density),
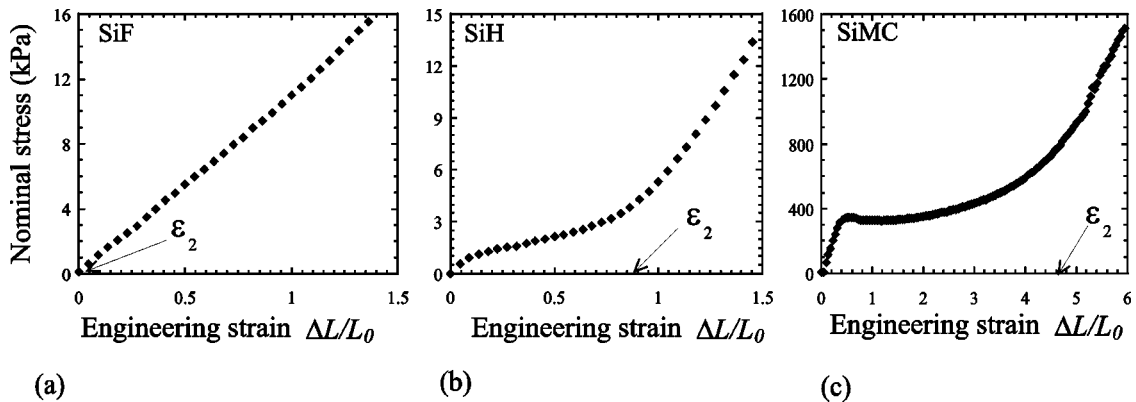

FIG. 5. Stress-strain curves for stretching perpendicular to the nematic director. For each of the three samples, the director is made to rotate towards the stretching axis, producing a soft stress plateau. The slopes of each plot before the soft threshold ε_1 give an estimate for the Young modulus $E_{\perp}$ for SiF: 11 kPa (at 24C), SiH: 12 kPa (at 30C), and SiMC: 0.86 MPa (at 60.9C). The calculated strain range of the soft plateau ε_2 is labeled on each graph.
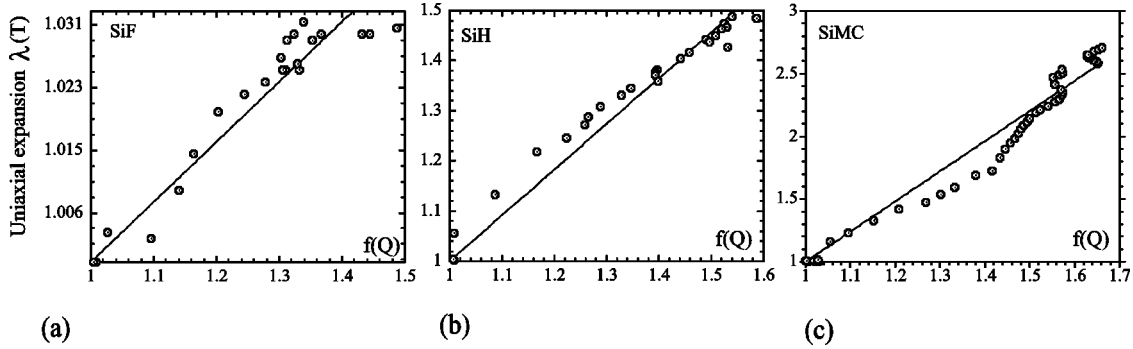
FIG. 6. The spontaneous uniaxial strain $\lambda_{th}=L/L_0$, increasing on cooling, is plotted parametrically against the function of order-parameter $f(Q)$, see text. All three samples, SiF, SiH, and SiMC, are following the linear relation, $\lambda_{th}=1+\beta[f(Q)-1]$, but with a very different slope: the fitted line gives $\beta=0.079, 0.9, 2.4$ for the three samples, respectively.

where the anisotropy r was reasonably high but the rates of stress and shape relaxation still manageable.

The isotropic-nematic transition at T_{ni} is abrupt in all our materials, with no supercritical effects or paranematic phase. The nematic order-parameter $Q(T)$ has very nearly the same values and temperature dependence in all materials studied. The simplest molecular model of nematic polymers, based on the freely jointed chain of rods, gives the prediction for step lengths, $\ell_{\parallel}=a(1+2Q)$ and $\ell_{\perp}=a(1-Q)$, which gives the dimensionless ratio $r=(1+2Q)/(1-Q)$ with no additional parameter dependence. The ideal theory predicts that $\lambda_{th}=r^{1/3}$. Accordingly, in Fig. 6, we attempt to plot the variation of spontaneous uniaxial thermal expansion $\lambda=L/L_0$ against the function of nematic order-parameter $f(Q)=[(1+2Q)/(1-Q)]^{1/3}$, for SiF, SiH, and SiMC. The linear relation between these two functions of temperature is impressive. However, one cannot forget that the freely jointed chain model predicts a coefficient of exact unity, that is $\lambda=f(Q)$. Instead, we find in Fig. 6 that there is a strongly varying multiplicative factor in the linear proportionality: $\lambda=1+\beta\times[f(Q)-1]$. The slope for weakly anisotropic elastomer SiF is $\beta\approx0.079$, for SiH we find an almost exact equality $\beta\approx0.9$ and the highly anisotropic SiMC has the slope $\beta\approx2.4$. Of course, there is no possible connection with the freely jointed chain model (which does not leave any freedom of parameters) and the relationship $\lambda=f(Q)$ found in [16] [very similar to the result in Fig. 6(b) for SiH] should be regarded as coincidental. Clearly, the cross-linking geometry and conditions have a profound effect on the resulting monodomain nematic elastomer.

An alternative, but equally correct way of looking at the role of nematic order parameter is to introduce a separate "nematic" order of the polymer backbone, which forms the elastic network. Such a parameter Q_b may be directly determined from the measured mechanical anisotropy $r=(1+2Q_b)/(1-Q_b)$, or

$$Q_b\equiv\frac{r-1}{r+2}.$$

The linear relationship between Q_b and the main spontaneous nematic order parameter $Q(T)$ is demonstrated in Fig. 7 for the three materials under study. It is a comforting result, even though slightly unexpected for such a wide range of materials and temperatures below T_{ni}.

The study of mechanical actuation, that is the contraction and elongation under changing conditions (in our case—temperature), and thus exerting a force, shows that uniformly aligned nematic elastomers have a great potential in practical applications, from stress and deformation gauges, to artificial muscles and micromanipulators. On the map of material properties of different materials used in actuator design [22], the nematic elastomers would occupy the region of low stress (unlikely to exceed a few MPa) and extremely high deformations. In comparison, the present "large-amplitude" actuators are based on shape-memory alloys, which reach strains of up to 10%—something that pales in comparison with over 300% deformations described in this paper.
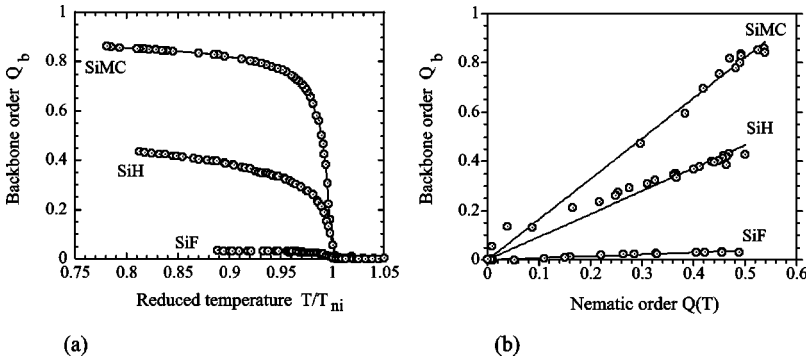

FIG. 7. The effective backbone order-parameter Q_b plotted (a) against the reduced temperature T/T_{ni} and (b) parametrically against the main nematic order-parameter $Q(T)$, for the three samples, SiF, SiH, and SiMC (labeled on plots). The solid lines show the linear fits with the slope of 1.64, 0.93, and 0.08, respectively.

---

[1] W. Gleim and H. Finkelmann, in *Side-Chain Liquid Crystal Polymers*, edited by C. B. McArdle (Blackie, London, 1989).

[2] G. G. Barclay and C. K. Ober, Prog. Polym. Sci. **18**, 899 (1993).

[3] H. R. Brand and H. Finkelmann, in *Handbook of Liquid Crystals*, edited by D. Demus *et al.*, (Wiley-VCH, New York 1998).

[4] E. M. Terentjev, J. Phys.: Condens. Matter **11**, R239 (1999).

[5] M. Warner and E. M. Terentjev, Prog. Polym. Sci. **21**, 853 (1996).

[6] S. Kutter and E. M. Terentjev, e-print cond-mat/0106193 [Eur. Phys. J. E (to be published)].

[7] J. Küpfer and H. Finkelmann, Macromol. Chem. Phys. **195**, 1353 (1994).

[8] J. Schätzle, W. Kaufhold, and H. Finkelmann, Macromol. Chem. Phys. **190**, 3269 (1989).

[9] N. Assfalg and H. Finkelmann, Kaut. Gummi. Kunstst. **52**, 677 (1999).

[10] A. R. Tajbakhsh and E. M. Terentjev, cond-mat/0106138 [Eur. Phys. J (to be published)].

[11] M. Warner, P. Bladon, and E. M. Terentjev, J. Phys. II **4**, 91 (1994).

[12] S. V. Fridrikh and E. M. Terentjev, Phys. Rev. E **60**, 1847 (1999).

[13] X. J. Wang and M. Warner, J. Phys. A **19**, 2215 (1986).

[14] I. Kundler and H. Finkelmann, Macromol. Chem. Phys. **199**, 677 (1998).

[15] S. M. Clarke and E. M. Terentjev, Phys. Rev. Lett. **81**, 4436 (1998).

[16] H. Finkelmann, A. Greve, and M. Warner, Eur. Phys. J. E **5**, 281 (2001).

[17] V. Percec and M. Kawasumi, Macromolecules **24**, 6318 (1991).

[18] V. Castelletto, L. Noirez, and P. Vigoureux, Europhys. Lett. **52**, 392 (2000).

[19] J. P. Cotton and F. Hardouin, Prog. Polym. Sci. **22**, 795 (1997).

[20] F. Elias, S. M. Clarke, R. Peck, and E. M. Terentjev, Europhys. Lett. **47**, 442 (1999).

[21] G. R. Mitchell, F. Davis, and W. Guo, Phys. Rev. Lett. **71**, 2947 (1993).

[22] J. E. Huber, N. A. Fleck, and M. F. Ashby, Proc. R. Soc. London, Ser. A **453**, 2185 (1997).